Experimental Evaluation of a Procedure for SMF Continuity Plate and Weld Design

ADEL MASHAYEKH and CHIA-MING UANG

ABSTRACT

The AISC *Seismic Provisions* require that continuity plates in a special moment frame (SMF) welded moment connection be connected to the column flanges by complete-joint-penetration groove welds. Tran et al. (2013) have proposed a design procedure that allows the designer to evaluate the required forces in the continuity plates such that more economical welds (e.g., fillet welds) can be used; the required thickness of the continuity plates also need not be the same as that prescribed in the AISC *Seismic Provisions*. With some minor modifications to the original design procedure, two one-sided reduced beam section moment connection specimens were designed and constructed for experimental verification of the proposed design procedure. To evaluate the effect of potential column kinking on the fillet-welded joints between the continuity plates and the column flanges, weaker panel zones that still satisfied the code requirement were used. Although the AISC *Seismic Provisions* implicitly assume that continuity plates should remain essentially elastic, the continuity plate thickness of one specimen was intentionally undersized to evaluate the effect of continuity plate yielding on the connection performance. Test results showed that using fillet welds is feasible; no damage was observed in these fillet welds, and the connection performance was not affected by the type of weld joints used. The design procedure also indicates the significant effect of in-plane moment in the continuity plate's strength check, especially when shallow columns are used.

Keywords: special moment frames, reduced beam section, continuity plates, complete-joint-penetration weld, fillet weld.

INTRODUCTION

Beam-to-column moment connections play a vital role in the seismic performance of steel special moment frames (SMFs). Following capacity design principles, the intent of AISC 341-16, *Seismic Provisions for Structural Steel Buildings* (AISC, 2016a), is to ensure that system ductility is provided primarily through flexural yielding of beams, flexural yielding of columns at the base, and limited yielding of column panel zones. When beam flanges are directly connected to the column flanges in the strong-axis direction, continuity plates (i.e., transverse stiffeners) in the column, at the beam flange levels, are often needed to transfer the large concentrated beam flange forces to the column. Continuity plates also play an important role in reducing the stress concentration that occurs at the beam flange complete-joint-penetration (CJP) groove welds (FEMA 2000a, 2000b). AISC 341-16 requires that continuity plates be connected to the column flanges with CJP welds; groove welds or fillet welds can be used on the column web side. The requirement of CJP welds is based mainly on available test data, where almost all welded moment connection specimens tested in the United States—especially those tested after the 1994 Northridge, California, earthquake—were fabricated with this weld detail. Not having a mechanics-based design procedure that allows the designer to quantify the required forces in the continuity plates is another reason for requiring expensive CJP welds in AISC 341-16.

According to the 2010 AISC *Seismic Provisions*, AISC 341-10 (AISC, 2010a), continuity plates are not required when the column flange thickness, t_{cf}, meets the following two requirements:

$$t_{cf} \geq 0.4\sqrt{1.8 b_{bf} t_{bf} \frac{R_{yb} F_{yb}}{R_{yc} F_{yc}}} \quad (1)$$

$$t_{cf} \geq \frac{b_{bf}}{6} \quad (2)$$

where b_{bf} and t_{bf} are the beam flange width and thickness, F_{yb} and F_{yc} are the beam and column yield stresses, and R_{yb} and R_{yc} are the beam and column yield stress adjustment factors, respectively. When required, the continuity plate thickness shall be at least equal to 50 and 100% of the beam flange thickness for one-sided and two-sided connections, respectively. Note that Equation 1 is a carryover from older codes (ICBO, 1994), except for the R_y factors. Specifically, this equation was derived based on the assumption that the bolted beam web, as in pre-Northridge moment connections,

Adel Mashayekh, Ph.D., Staff 2 Structures, Simpson Gumpertz & Heger, Inc., San Francisco, CA. Email: amashayekh@sgh.com

Chia-Ming Uang, Ph.D., Professor, Department of Structural Engineering, University of California, San Diego, La Jolla, CA. E-mail: cmu@ucsd.edu (corresponding)

Paper No. 2017-03

was not effective in sharing a portion of the beam moment such that each beam flange would be strained to 1.8 times the beam flange yield strength (Bruneau et al., 2011). Equating this required beam flange force to the flange local bending strength of the column specified in Section J10.1 of AISC 360, *Specification for Structural Steel Buildings* (AISC, 2016c), results in Equation 1. Equation 2 was established based on low-cycle fatigue consideration (Ricles et al., 2000; FEMA, 2000b).

Two changes were made in AISC 341-16. First, the continuity plate thickness requirement is relaxed from 100% to 75% of the beam flange thickness for two-sided connections (Lee et al., 2005). Second, Equation 1 was eliminated and replaced by a more general requirement. For connections in which the beam flanges are welded to the column flange, the required beam flange force, P_b, can be computed from the maximum probable moment, M_f, at face of column as follows:

(a) When beam webs are bolted connected to the column:

$$P_b = \frac{M_f}{\alpha_s d^*} \tag{3}$$

(b) When beam webs are welded to the column:

$$P_b = \frac{0.85 M_f}{\alpha_s d^*} \tag{4}$$

where

M_f = maximum probable moment at face of column as defined in AISC 358-16, *Prequalified Connections for Special and Intermediate Steel Moment Frames for Seismic Applications* (AISC, 2016b), for a prequalified moment connection or as determined from qualification testing

d^* = distance between centroids of beam flanges or beam flange connections to the face of the column

α_s = LRFD-ASD force level adjustment factor
= 1.0 for LRFD and 1.5 for ASD

The 0.85 factor in Equation 4 was based on Tran et al. (2013). The required beam flange force is then checked against all the applicable limit states stipulated in AISC 360-16, Section J10, to determine if continuity plates are needed.

In this paper, welds that connect a continuity plate to the column flanges and the web are referred to as the flange weld and web weld, respectively.

OBJECTIVE

Although some improvements have been made in AISC 341-16, the design of continuity plates and their welds is still prescriptive in nature. That is, the thickness of continuity plate is prescribed, and a CJP weld is required for the flange weld. Based on the relative stiffness (or flexibility) between the column flange being pulled out of its plane and the continuity plates being loaded mainly in shear in its own plane by the beam flange force, Tran et al. (2013) developed a flexibility-based procedure that allows the designer to calculate the required forces in both the continuity plate as well as flange and web welds, thus providing more freedom to size the thickness and design welded joints for the continuity plates. The objective of this study was to provide an experimental verification of this proposed design procedure.

PROPOSED DESIGN PROCEDURE

The procedure proposed by Tran et al. (2013) and subsequently modified in this study is summarized herein. Representing the beam flange force as

$$P_b = C_{pf} R_{yb} b_{bf} t_{bf} F_{yb} \tag{5}$$

AISC 341-10 assumed that the beam flange force adjustment factor, C_{pf}, was equal to 1.8 to establish the minimum column flange thickness requirement shown in Equation 1. While this assumed value is reasonable for pre-Northridge–type welded flange-bolted web moment connections, where the bolted web is ineffective in contributing to the moment resistance, Tran et al. showed that this assumption, and hence Equation 1, is conservative for some post-Northridge moment connections like the reduced beam section (RBS) or welded unreinforced flange-welded web (WUF-W) moment connections in AISC 358, where the beam web is directly welded to the column flange with a CJP weld. Based on finite element analysis, the following C_{pf} values were recommended by Tran et al.:

For RBS connection: $C_{pf} = 1.25$ (6a)

For WUF-W connection: $C_{pf} = 1.75$ (6b)

When continuity plates are required, the beam flange axial force, P_b, is apportioned to each continuity plate based on the following equation (Tran. et al., 2013):

$$P_{cp} = \frac{P_b}{2}\left(\frac{b_{bf} - t_{pz} - 2t_{cf}}{b_{bf}}\right)\left(\frac{B_{cf}}{B_{cf} + B_{cp}}\right) \tag{7}$$

where

B_{cf} = column flange out-of-plane flexibility coefficient

B_{cp} = continuity plate in-plane flexibility coefficient

P_{cp} = normal force transmitted to one continuity plate

b_{bf} = beam flange width

t_{cf} = column flange thickness

t_{pz} = panel zone thickness

(See Tran et al. for the derivation of Equation 7.) Following the procedure, the required forces can be computed along three edges of the continuity plate. To ensure that

the continuity plates have sufficient in-plane stiffness, the designer then checks the available column strength determined using the applicable limit states stipulated in AISC 360-16, Section J10 for the portion of the beam flange force that will be transmitted from the beam flange to the column web directly:

$$P_b - 2P_{cp} \le \phi R_n \tag{8}$$

Figure 1 shows that the edges of the continuity plate next to the loaded column flanges are subjected to both normal and shear forces, where the shear force from moment equilibrium is:

$$V_{cp} = \left(\frac{0.6b}{d}\right)\sum P_{cp} \tag{9}$$

The Von-Mises yield criterion is then used by Tran et al. (2013) to check the strength of the continuity plates:

$$\left(\frac{P_{cp}}{F_{ycp}A_n}\right)^2 + \left(\frac{V_{cp}}{\frac{F_{ycp}}{\sqrt{3}}A_n}\right)^2 \le 1 \tag{10}$$

where

A_n = $b_n t_{cp}$
F_{ycp} = yield stress of continuity plate
b = $b_{clip} + b_n$ (total width of continuity plate)
b_{clip} = corner clip size
b_n = net width of continuity plate
d = depth of continuity plate
t_{cp} = thickness of continuity plate

When Equation 9 is satisfied, either fillet welds or partial-joint-penetration groove welds can be used to connect the continuity plates to the column flanges. If not, Tran et al. (2013) suggested that CJP groove welds still be used because continuity plates are expected to yield. To avoid the use of CJP welds, however, an alternative is to increase the thickness of the continuity plates such that Equation 9 is satisfied.

In designing the specimens for this test program, some modifications were made to Equation 9. By ignoring the corner clips in the continuity plates in finite element analysis, Tran et al. (2013) suggested that the normal force, P_{cp}, be located at a distance $0.6b$ from the column web (see Figure 1); the moment produced by this force with an eccentricity with respect to the center of the net width of the continuity plate was ignored in checking the strength in Equation 9. To include the moment component, Dowswell (2015) suggested an *M-V-P* yield criterion, which can be rewritten as the following:

$$\left(\frac{P_{cp}e}{Z_{xn}F_{ycp}}\right) + \left(\frac{P_{cp}}{F_{ycp}A_n}\right)^2 + \left(\frac{V_{cp}}{\frac{F_{ycp}}{\sqrt{3}}A_n}\right)^4 \le 1 \tag{11}$$

where Z_{xn} is the plastic section modulus of the net section:

$$Z_{xn} = \frac{t_{cp}b_n^2}{4} \tag{12}$$

Refer to Figure 2(a) for a continuity plate in a two-sided (i.e., interior) moment connection, where corners are clipped to clear the *k*-area of the column section. Free-body diagram 3 in Figure 2(c) shows that the normal force P_{cp} acts at a distance $0.6b$ from the column web, and moment equilibrium requires that

$$V_{cp} = \left(\frac{0.6b}{d - 2b_{clip}}\right)\sum P_{cp} \tag{13}$$

Next consider free-body diagram 1 or 2. The corner clip causes the normal force at the edge of the net width to shift by an amount e^* to satisfy moment equilibrium:

$$e^* = \frac{b_{clip}V_{cp}}{P_{cp}} \tag{14}$$

Therefore, the moment produced by the eccentrically loaded P_{cp} at the center of the net width equals eP_{cp}, where

$$e = 0.6b + e^* - (b_{clip} + 0.5b_n) \tag{15}$$

The same approach can be applied to the continuity plate of a one-sided (i.e., exterior) moment connection. But the shear force calculation needs to be modified slightly.

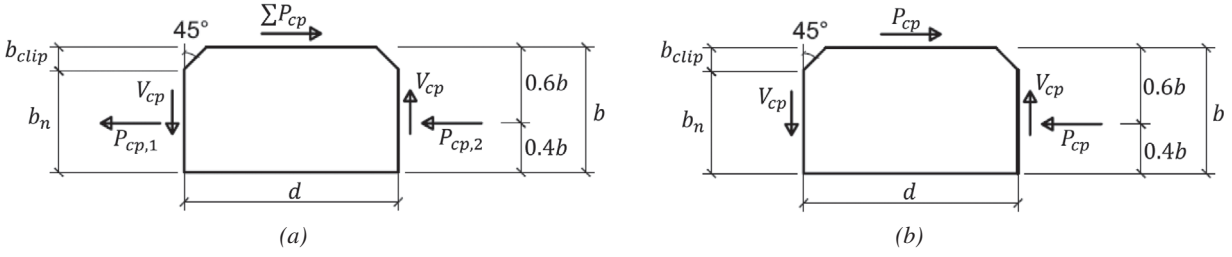

Fig. 1. Free-body diagram of a continuity plate: (a) interior connection; (b) exterior connection (Tran et al., 2013).

As shown in Figure 3, it is assumed that the normal force at the nonloaded column flange side of the continuity plate equals zero. Therefore, the shear force is

$$V_{cp} = \left(\frac{0.6b}{d - b_{clip}} \right) P_{cp} \tag{16}$$

and Equation 11, not Equation 9, was used to design the continuity plates in this test program.

TEST PROGRAM

Two full-scale RBS connection specimens were tested. Figure 4 shows the member sizes and specimen dimensions. Specimen C1 had a W30×116 beam connected to a deep column (W24×176), while a W36×150 beam was connected to a shallow column (W14×257) for specimen C2. Table 1 summarizes the steel mechanical properties; ASTM

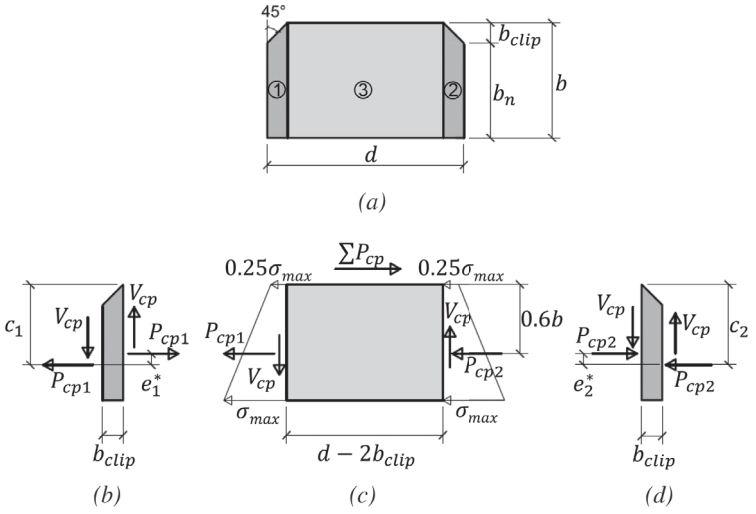

Fig. 2. Continuity plate free-body diagrams (interior connection): (a) geometry of continuity plate; (b) free-body 1; (c) free-body 3; (d) free-body 2.

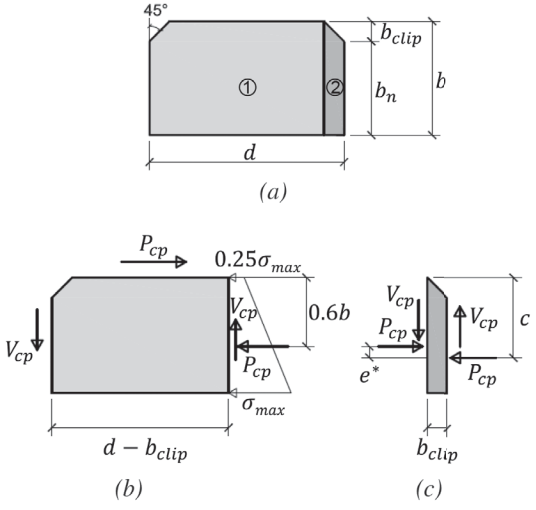

Fig. 3. Continuity plate free-body diagrams (exterior connection): (a) geometry of continuity plate; (b) free-body 1; (c) free-body 2.

A992 steel was specified for the beams and columns, and ASTM A572 Grade 50 steel was specified for the continuity plates. Figure 5 depicts the RBS dimensions and the weld details. Except for the continuity plates and their welds, both specimens were designed in accordance with AISC 341-10 (AISC, 2010a) and AISC 358-10 (AISC, 2010b). No doubler plates were required per AISC 341-10.

Member sizes as well as RBS dimensions were selected such that the demand-capacity ratios for the panel zone shear were high (0.9 and 0.95 for specimens C1 and C2, respectively). The intent of such design was to produce a large panel-zone deformation to investigate if kinking of the column flanges would adversely affect the performance of fillet welds that connected the continuity plates to the column flanges.

The required forces in the continuity plates and the fillet weld sizes per the proposed procedure are provided in Table 2. The proposed design called for a continuity plate thickness of ⅞ in. for specimen C2. AISC 341 implicitly assumes that continuity plates should remain essentially elastic. Because the effect of yielded continuity plates had never been reported in the literature, it was decided to use ⅝-in.-thick continuity plates instead. A comparison of the welds for the continuity plates based on both AISC 341-10 and the proposed procedure is also provided in the table. Self-shielded, flux-cored arc welding with an E71T-8 electrode (Lincoln/Innershield NR 232) that met the demand critical requirement of AWS D1.8 (AWS, 2009) was used for making the welds.

Table 3 summarizes the components of Equation 11 for the design of both specimens. The continuity plates of specimen C2 were significantly undersized with a demand-capacity ratio of 1.31. The shear force component was minimal for the deep-column specimen C1, mainly because the denominator $(d - 2b_{clip})$ in Equation 13 was larger. For the shallow-column specimen C2, both shear and moment components are significant. Therefore, it is not appropriate to use Equation 9 to check the strength of continuity plates.

Lateral restraint was provided near the loaded beam end for both specimens. For specimen C1, which utilized a deep column, one extra restraint was provided at a distance 15.4 in. outside the RBS region to simulate the slab restraining effect. The loading sequence in AISC 341-16, Chapter K, expressed in terms of the story drift angle for beam-to-column moment connection testing was followed. A positive drift angle corresponded tothe beam end deflection upward.

TEST RESULTS

Figure 6 shows the global response of the test specimens. Both specimens performed well and met the AISC acceptance criteria, which require that (1) the connection shall accommodate a story-drift angle of at least 0.04 rad, and (2) the measured flexural strength of the beam shall equal at least 80% of the nominal plastic moment, M_{pn}, of the connected beam at a story-drift angle of 0.04 rad.

Figure 7 shows the yielding and buckling pattern of

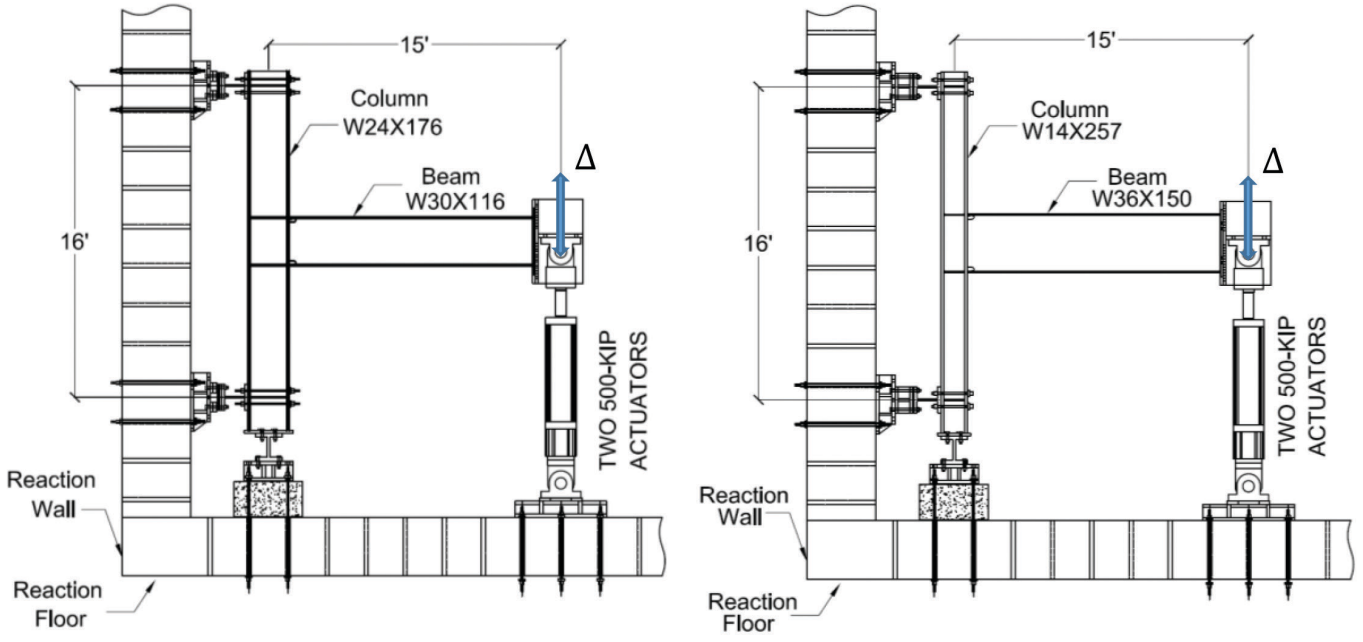

Fig. 4. Test specimens and test setup: (a) specimen C1; (b) specimen C2.

specimen C1; as expected, local buckling and lateral-torsional buckling in the beam as well as shear yielding in the panel zone were observed. Testing was stopped after completing one cycle at 5% story drift because the beam flexural strength at the column face had degraded below $0.8M_{pn}$. The panel zone of specimen C2 was designed with a higher demand-capacity ratio (0.95). Shear yielding of the panel zone was very significant (Figure 8). The panel zone shear yielding caused significant column flange kinking; localized column flange yielding due to such kinking is evidenced in Figure 9. Local buckling of the beam occurred at 4% drift, and lateral-torsional buckling was observed during the second cycle at 5% drift. One cycle at 7% drift was then imposed on the specimen before the test was stopped.

Figures 10 and 11 show the close-up views of the fillet welds connecting the continuity plates to the column flanges. Dye-penetrant testing was conducted on the fillet welds after the tests; no damage was observed. Note that significant kinking of the column flanges occurred at these weld locations for both specimens because the panel zones were intentionally designed to have large demand-capacity ratios. Figure 12 shows that the shear strain reached nine times the shear yield strain for specimen C2. The shear strain reached in specimen C1 was lower; the "unusual" nonlinear response shown in Figure 12(a) was due to twisting of the deep column (Chi and Uang, 2002).

Based on the flaking pattern of the whitewash in the connection region, it was observed that the continuity plates of specimen C2 yielded, while those of specimen C1 remained elastic; measured strains (to be presented later) further confirm this observation. Although significant yielding occurred in the continuity plates of specimen C2 due to the intentional undersize of the plate thickness, the connection performance was not affected.

Beam flanges and continuity plates were instrumented with strain gages and rosettes (see Figure 13). The measured

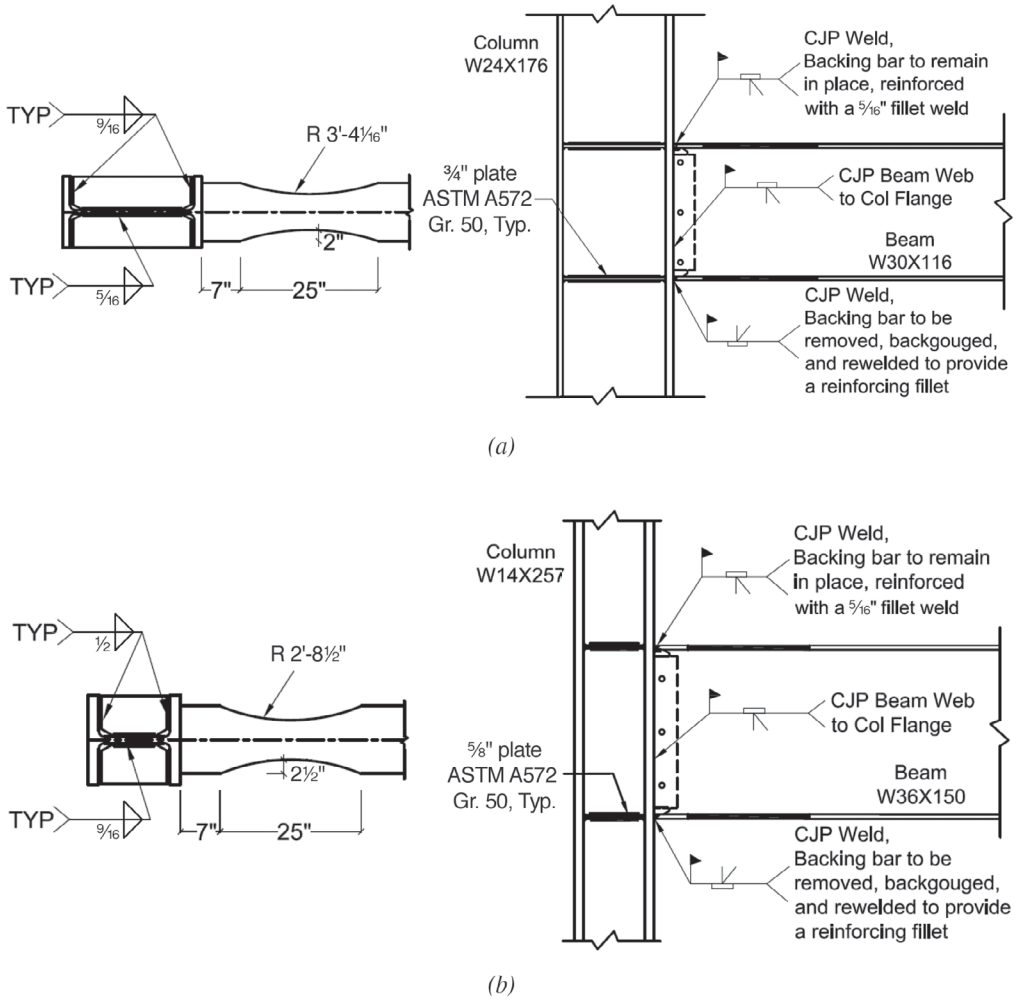

Fig. 5. RBS connection details: (a) specimen C1; (b) specimen C2.

Table 1. Steel Mechanical Properties				
Specimen No.	**Component**	**Yield Stress (ksi)**	**Tensile Strength (ksi)**	**Elongation (%)**
C1	Beam flange	56.9	75.6	34.5
	Beam web	58.5	73.2	39.5
	Column flange	57.2	70.6	39.1
	Column web	58.5	72.2	37.3
	Continuity plate	68.1	85.6	36.9
C2	Beam flange	53.5	74.9	38.3
	Beam web	57.9	74.7	38.1
	Column flange	52.3	74.3	37.7
	Column web	54.8	74.8	38.6
	Continuity plate	54.1	79.8	35.1

Table 2. Continuity Plate and Weld Design				
	Specimen C1		**Specimen C2**	
	Proposed Procedure	**AISC 341-16**	**Proposed Procedure**	**AISC 341-16**
Required continuity plate forces (kips)	$P_{cp} = 157.6$ $V_{cp} = 26.7$	N.A.	$P_{cp} = 157.0$ $V_{cp} = 62.8$	N.A.
Continuity plate thickness	¾ in.	½ in. (= $t_{bf}/2$)	⅝ in.	½ in. (= $t_{bf}/2$)
Continuity plate-to-column flange weld	Fillet weld (⅝ in.)	CJP weld	Fillet weld (½ in.)	CJP weld
Continuity plate-to-column web weld	Fillet weld (⅝ in.)	Fillet weld (⅜ in.)	Fillet weld (⅝ in.)	Fillet weld (⅜ in.)

Table 3. Continuity Plate Strength Check				
	Equation 11			
Specimen No.	**Moment Component,** $\left(\frac{P_{cp}e}{Z_{xn}F_{ycp}}\right)$	**Normal Force Component,** $\left(\frac{P_{cp}}{F_{ycp}A_n}\right)^2$	**Shear Force Component,** $\left(\frac{V_{cp}}{\frac{F_{ycp}}{\sqrt{3}}A_n}\right)^4$	**Σ**
C1	0.14	0.78	0.01	0.93
C2	0.36	0.80	0.15	1.31

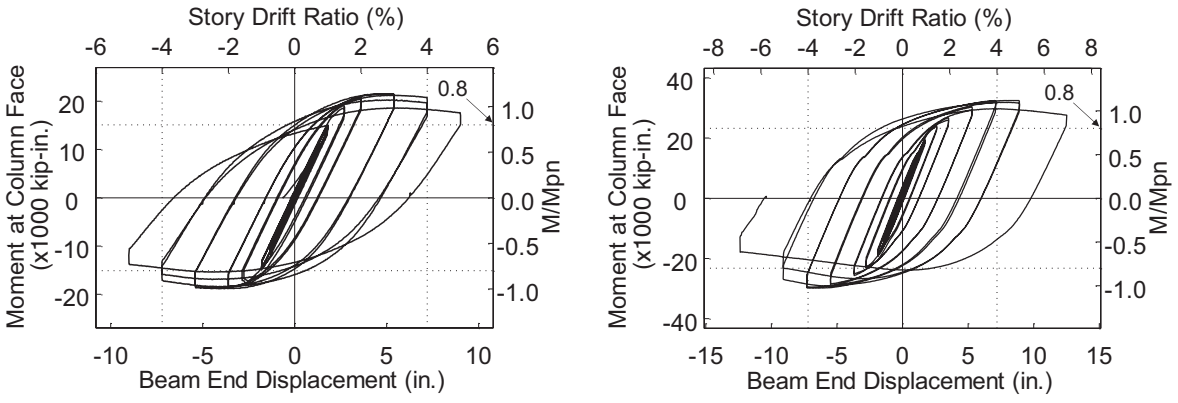

Fig. 6. Global responses: (a) specimen C1; (b) specimen C2.

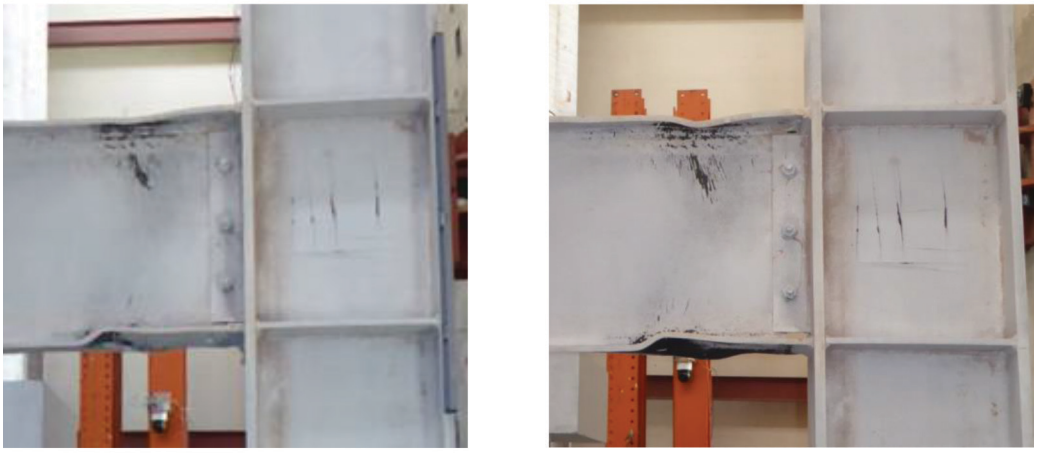

Fig. 7. Global view of specimen C1: at 0.04-rad drift (second cycle); (b) at test completion.

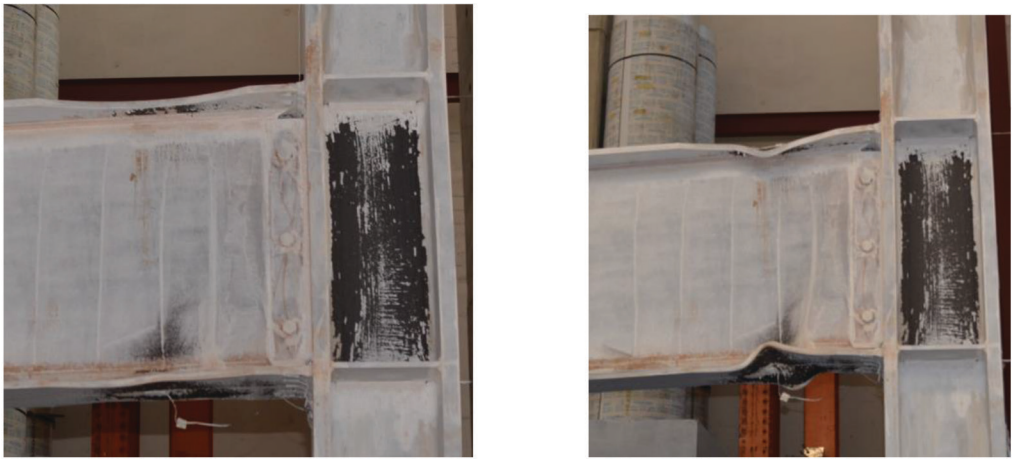

Fig. 8. Global view of specimen C2: (a) at 0.04-rad drift (second cycle); (b) at 0.07-rad drift (first cycle).

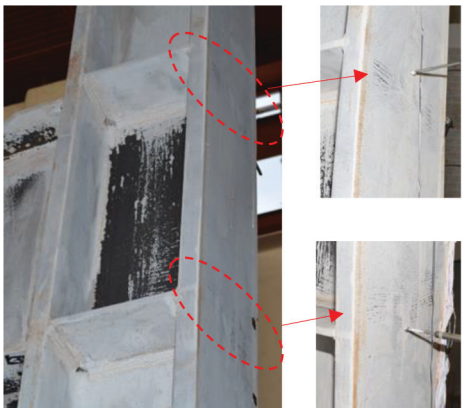

Fig. 9. Specimen C2 localized column flange yielding due to panel zone deformation.

(a) *(b)*

Fig. 10. Fillet welds of specimen C1 after test: (a) beam top flange level; (b) beam bottom flange level.

(a) *(b)*

Fig. 11. Fillet welds of specimen C2 after test: (a) beam top flange level; (b) beam bottom flange level.

normal and shear strains, after normalizing by their respective yield strains, of specimen C2 at 4% story drift are presented in Figure 14. Only one continuity plate was instrumented. For clarity, however, the normalized shear strain distributions are plotted on the other continuity plate. At a distance 3 in. away from the loaded column flange, the beam flange flexural strains reached $3.5\varepsilon_y$, where ε_y is the yield strain. On the opposite side of the loaded column flange, the continuity plate also yielded for the reason mentioned earleir; the maximum normal strain, which occurred near the free edge of the continuity plate, reached $2.63\varepsilon_y$. Along the length of the flange weld, the profile of the strain normal to the weld was consistent with that proposed by Tran et al. (2013).

Figure 14 also shows that shear strains of the continuity plate along the length of the same flange weld were high; the maximum shear strain reached $1.56\gamma_y$, where γ_y is the shear yield strain. The maximum shear strain occurred near the column web, not the free edge of the continuity plate, which is also consistent with that proposed by Tran et al. (2013), Along the length of the web weld—that is, along the column web—the shear strain reached a maximum value of $1.88\gamma_y$ at the loaded column flange end. This uneven strain distribution reflects the effect of the short distance in a shallow (W14) column that a portion of the beam flange force needed to be transferred from the continuity plate through the column web to the panel zone.

The normal strain from strain rosette R1 near the nonloaded column flange was about 0.6 times that of the strain of R6 near the loaded column flange, which indicates that a significant portion of the force was still transmitted through the continuity plate to the nonloaded column flange. Therefore, it is prudent to use the same weld size for both flange welds.

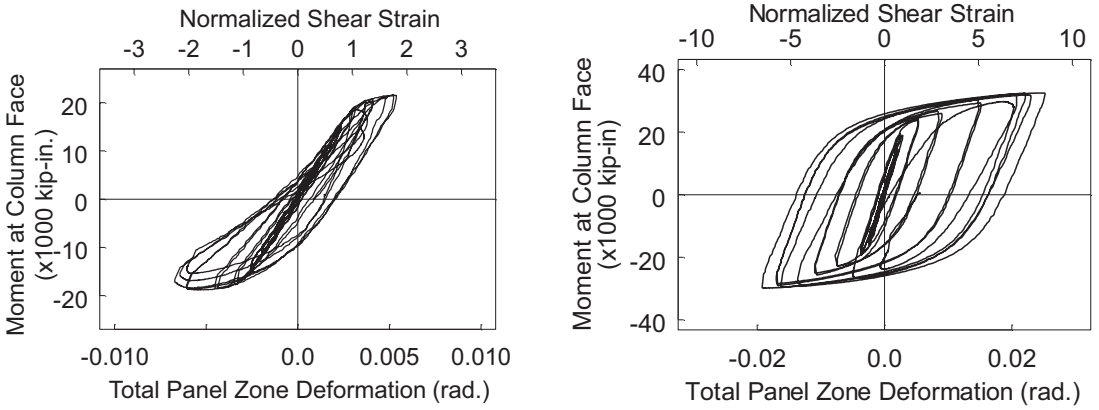

Fig. 12. Measured panel zone responses: (a) speciment C1; (b) specimen C2.

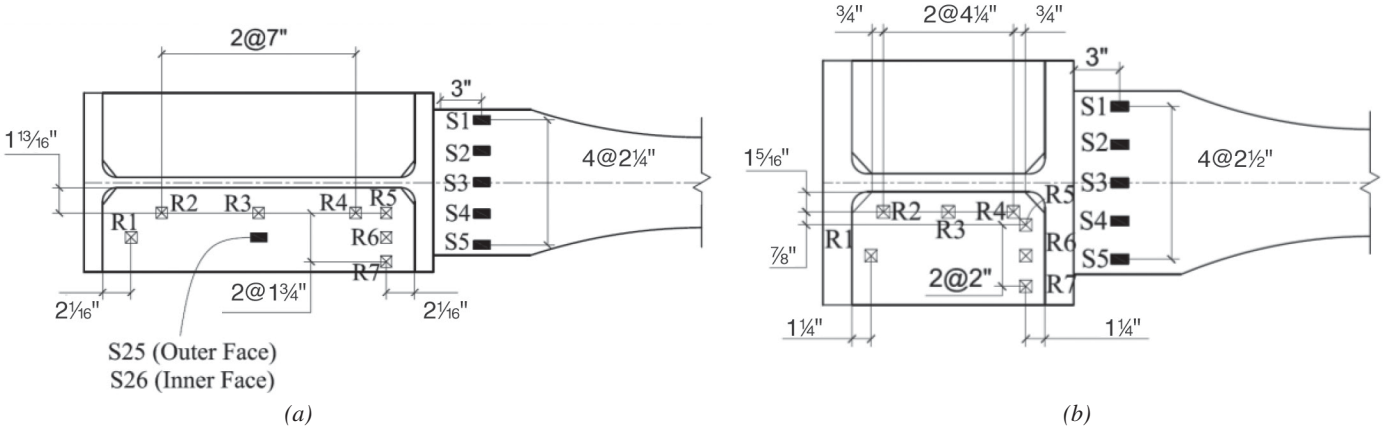

Fig. 13. Strain gage and rosette layout (beam top flange level): (a) specimen C1; (b) specimen C2.

Specimen C1 had a deep (W24) column, which experienced twisting due to lateral-torsional buckling of the beam and affected strain readings. Based on the readings of the strain gages that were placed on the loaded column flange, column twisting became significant beyond 1.5% drift when warping stresses started to affect flexural strains in the column flange. Therefore, measured strains of a continuity plate at the top flange level at 1.5% drift are presented. At this load level, which was about 86% that of the peak load experienced by this specimen, Figure 15 shows that the magnitude of the continuity plate normal strains perpendicular to the flange weld was similar to that of the beam flange strains. From the free-body diagram in Figure 1, the force couple produced by the shear force V_{cp} along each flange weld is needed to satisfy moment equilibrium; the shear force is smaller relative to the normal force P_{cp} when the column is deep because the level arm is larger. This is indeed observed in Figure 15, where the normalized shear strain along the flange weld was significantly smaller than that in Figure 14. In a deep column, a longer distance along the column web is available to transmit the P_{cp} force through the web weld to the panel zone. This explains why the shear strain distribution along the web weld is more uniform than that in Figure 14.

FINITE ELEMENT ANALYSES

It is difficult to experimentally construct the free-body diagram of the continuity plate from strain gage measurements. Instead, finite element analysis (FEA) by using the commercial software ABAQUS (2014) was conducted. Free-body diagrams established from the FEA are then compared with those established from the proposed procedure.

Four-node, thick-shell brick elements (type S4R in ABAQUS) were used to model the specimens. Typical steel properties (E = 29,000 ksi, ν = 0.3) were used in the model to describe elastic material characteristics. Also for inelastic behavior, following the work of Chaboche (1986), material parameters that can simulate both the kinematic and isotropic hardening responses of an ASTM A992/A572 steel coupon under cyclic loading were incorporated. Figure 16 compares the experimental and predicted global response of each specimen; the correlation is satisfactory.

Figures 17 and 18 compare the free-body diagrams of two specimens. For these two one-sided moment connections, the proposed procedure assumes that the left (i.e., the nonloaded column flange) side has no normal force; the normal force from the beam flange is transferred completely to the column web through the continuity plate. The FEA shows that the nonloaded column flange does resist a portion of the

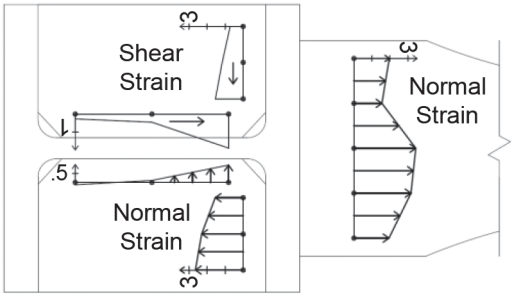

Fig. 14. Specimen C2 beam top flange and continuity plate normalized strain distributions (4% story drift).

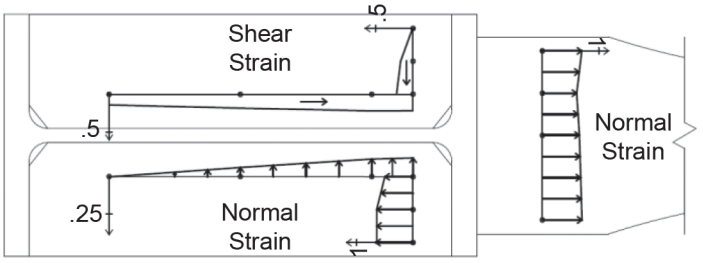

Fig. 15. Specimen C1 beam top flange and continuity plate normalized strain distributions (1.5% story drift).

normal force from the beam flange; the percentage is higher for shallow columns than for deep columns. This will reduce the shear force in the web weld. Because the proposed procedure assumes that all normal force from the beam flange is transmitted to the column web, the web weld design is somewhat conservative. These two figures also show that the shear force along the flange weld is larger when a shallow column is used.

SUMMARY AND CONCLUSIONS

AISC 341-16 requires that continuity plates in an SMF be connected to the column flanges by CJP welds. Tran et al. (2013) have proposed a design procedure that considers the in-plane flexibility (or stiffness) of the continuity plate relative to the out-of-plane flexibility of the column flange being loaded by the beam flange in determining the forces that are transmitted through the continuity plates to the column panel zone. As a pilot study to experimentally verify this design procedure, two full-scale reduced beam section (RBS) connection specimens were tested. Using a slightly modified procedure of that originally proposed by Tran et al., continuity plates in both specimens were fillet-welded to the column flanges. One specimen (C1) used a deep (W24) column, and the other (C2) had a shallow (W14) column. The continuity plate thickness of specimen C2 was undersized to evaluate the effect of yielded continuity plates on the connection performance. While still satisfying the code requirement, the demand-capacity ratio of the panel zone was high (0.90 and 0.95 for C1 and C2, respectively) in order to evaluate the effect of column flange kinking due to significant panel zone yielding on the performance of the fillet welds.

Based on the test results and the associated analytical studies, the following conclusions can be drawn:

1. Both specimens performed very well and met the 0.04-rad story-drift requirement specified in AISC 341-16. As expected, yielding and buckling in the RBS region, as well as significant shear yielding in the panel zone, were observed.
2. Fillet welds designed per the proposed design procedure that connected continuity plates to the column flanges did not show any damage. Therefore, CJP welds as required by AISC 341-16 may not always be necessary.
3. AISC 341-10 specifies a prescriptive requirement for the thickness of the continuity plates: half and full thickness of the beam flange for the exterior and interior moment connections, respectively. (The full thickness requirement has been changed to three-quarter thickness for the interior connection in AISC 341-16.) Test results showed that such a prescriptive requirement may not be needed; the proposed procedure will consider directly the effect of thickness on the forces transmitted to the continuity plates.
4. Edges of the continuity plates connecting to the column flanges are subjected to not only normal force, but also to shear force and moment; the moment is produced by the normal force with an eccentricity (Figures 2 and 3). The moment was ignored by Tran et al. (2013) in the strength check of the continuity plate (Equation 9). The revised procedure used to design the specimens in this study considered the moment effect (Equation 11). The effect of moment and shear can be significant, especially for continuity plates in shallow columns (Table 3).
5. AISC 341-16 implicitly assumes that continuity plates shall remain essentially elastic per the capacity design principles. Because the effect of plate yielding has never been reported in the literature, the plate thickness

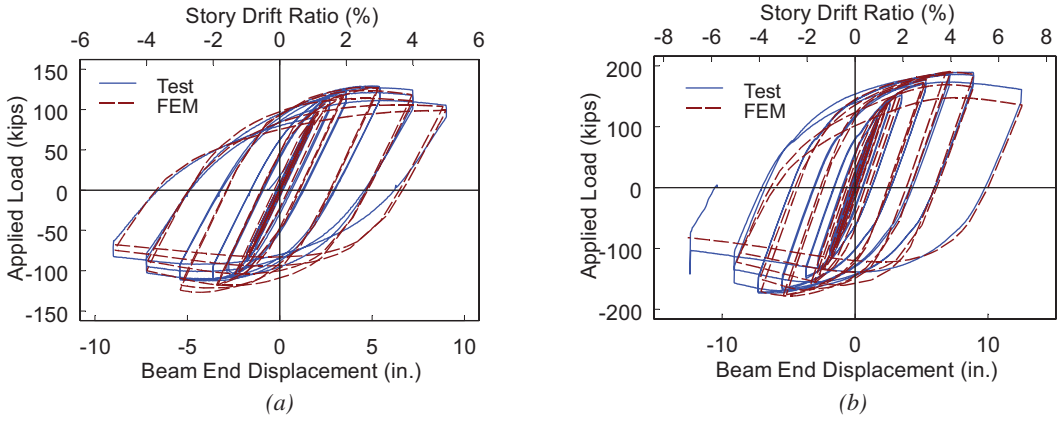

Fig. 16. Correlation of Global Responses: (a) specimen C1; (b) specimen C2.

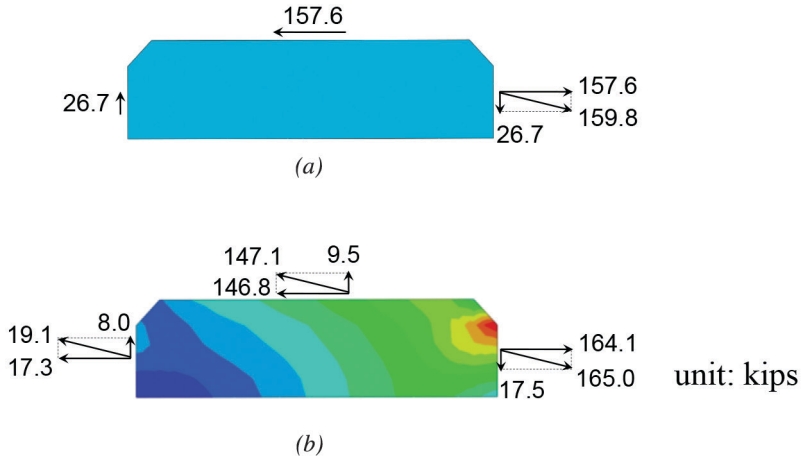

Fig. 17. Specimen C1—comparison of continuity plate free-body diagram: (a) proposed procedure; (b) finite element analysis.

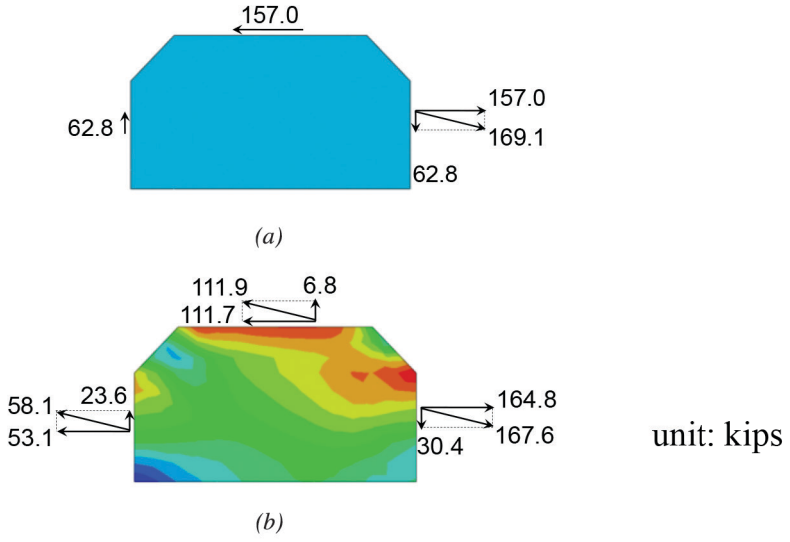

Fig. 18. Specimen C2—comparison of continuity plate free-body diagram: (a) proposed procedure; (b) finite element analysis.

of one specimen (C2) was undersized. Testing did show significant yielding in the plates, but connection performance was not affected.

ACKNOWLEDGMENTS

This project was sponsored by the American Institute of Steel Construction (AISC); Mr. Tom Schlafly served as the project manager for this research. Schuff Steel Company donated the test specimens. AMEC Foster Wheeler in San Diego provided inspection services to this project. Mr. Patrick M. Hassett of Hassett Engineering Inc. reviewed the design of the test specimens.

REFERENCES

ABAQUS (2014), *ABAQUS Standard User's Manual*, Version 6.14, ABAQUS Inc.

AISC (2010a), ANSI/AISC 341-10, *Seismic Provisions for Structural Steel Buildings*, American Institute of Steel Construction, Chicago, IL.

AISC (2010b), ANSI/AISC 358-10, *Prequalified Connections for Special and Intermediate Steel Moment Frames for Seismic Applications,* American Institute of Steel Construction, Chicago, IL.

AISC (2016a), ANSI/AISC 341-16, *Seismic Provisions for Structural Steel Buildings*, American Institute of Steel Construction, Chicago, IL.

AISC (2016b), ANSI/AISC 358-16, *Prequalified Connections for Special and Intermediate Steel Moment Frames for Seismic Applications,* American Institute of Steel Construction, Chicago, IL.

AISC (2016c), ANSI/AISC 360-16, *Specification for Structural Steel Buildings*, American Institute of Steel Construction, Chicago, IL.

AWS (2009), *Structural Welding Code-Seismic Supplement*, AWS D1.8/D1.8M, American Welding Society, Miami, FL.

Bruneau, M., Uang., C.-M. and Sabelli, R. (2011), *Ductile Design of Steel Structures*, 2nd Ed., McGraw-Hill, New York, NY.

Chaboche, J.L. (1986), "Time-Independent Constitutive Theories for Cyclic Plasticity," *International Journal of Plasticity*, Vol. 2, No. 2, pp. 149–188.

Chi, B. and Uang, C.-M. (2002), "Cyclic Response and Design Recommendations of Reduced Beam Section Moment Connections with Deep Columns," *Journal of Structural Engineering*, ASCE, Vol. 128, No. 4, pp. 464–473.

Dowswell, B. (2015), "Plastic Strength of Connection Elements," *Engineering Journal*, AISC, Vol. 52, No. 1, pp. 47–66.

FEMA (2000a), "Recommended Seismic Design Criteria for New Steel Moment-Frame Buildings," FEMA 350, Federal Emergency Management Agency, Washington, DC.

FEMA (2000b), "State-of-the-Art Report on Connection Performance," FEMA-355D, Federal Emergency Management Agency, Washington, D.C.

ICBO (1994), *Uniform Building Code*, International Conference of Building Officials. Whittier, CA.

Lee, D., Cotton, S.C., Hajjar, J.F. and Dexter, R.J. (2005), "Cyclic Behavior of Steel Moment-Resisting Connections Reinforced by Alternative Column Stiffener Details I. Connection Performance and Continuity Plate Detailing," *Engineering Journal*, AISC, Vol. 42, No. 4, pp. 189–213.

Ricles, J.M., Mao. C., Lu, L.W. and J. Fisher, J.W. (2000), "Development and Evaluation of Improved Details for Ductile Welded Unreinforced Flange Connections," SAC BD 00-24, SAC Joint Venture, Sacramento, CA.

Tran, A.T., Hasset, P.M. and Uang, C.-M. (2013), "A Flexibility-Based Formulation for the Design of Continuity Plates in Steel Special Moment Frames," *Engineering Journal*, AISC, Vol. 50, No. 3, pp. 181–200.